

1 **Is there an optimal ENSO pattern that enhances large-scale atmospheric**  
2 **processes conducive to tornado outbreaks in the U.S?**

3  
4  
5 Sang-Ki Lee<sup>1,2</sup>, Robert Atlas<sup>2</sup>, David Enfield<sup>1,2</sup>, Chunzai Wang<sup>2</sup>, and Hailong Liu<sup>1,2</sup>

6 <sup>1</sup>Cooperative Institute for Marine and Atmospheric Studies, University of Miami, Miami,  
7 Florida, USA

8 <sup>2</sup>Atlantic Oceanographic and Meteorological Laboratory, NOAA, Miami Florida, USA  
9 USA

10  
11  
12  
13  
14  
15  
16 November 2011

17  
18  
19  
20  
21  
22 Corresponding author address: Dr. Sang-Ki Lee, NOAA/AOML, 4301 Rickenbacker Causeway,  
23 Miami, FL 33149, USA. E-mail: [Sang-Ki.Lee@noaa.gov](mailto:Sang-Ki.Lee@noaa.gov).

1 **Abstract**

2 The record-breaking U.S. tornado outbreaks in the spring of 2011 prompt the need to identify  
3 long-term climate signals that could potentially provide seasonal predictability for intense U.S.  
4 tornado outbreaks. Here we use both observations and model experiments to show that a positive  
5 phase of Trans-Niño, characterized by cooling in the central tropical Pacific and warming in the  
6 eastern tropical Pacific, may be one such climate signal. The warming in the eastern tropical  
7 Pacific increases convection locally, but also contributes to suppressing convection in the central  
8 tropical Pacific. This in turn works constructively with cooling in the central tropical Pacific to  
9 force a strong and persistent teleconnection pattern in spring that increases both the upper-level  
10 westerly and lower-level southeasterly over the central and eastern U.S. These anomalous winds  
11 bring more cold and dry upper-level air from the high-latitudes and more warm and moist lower-  
12 level air from the Gulf of Mexico converging into the U.S. east of the Rocky Mountains, and also  
13 increase the lower-level vertical wind shear therein, thus providing large-scale atmospheric  
14 conditions conducive to intense tornado outbreaks over the U.S. A distinctive feature in the 2011  
15 Trans-Niño event is warming in the western tropical Pacific that further aided to suppress  
16 convection in the central tropical Pacific and thus contributed to strengthening the teleconnection  
17 response in the central and eastern U.S. in favor of increased U.S. tornado activity.

18  
19  
20  
21  
22  
23

1 **1. Introduction**

2 In April and May of 2011, a record breaking 1,061 tornadoes and 539 tornado-related  
3 fatalities were confirmed in the U.S., making 2011 one of the deadliest tornado years in U.S.  
4 history [<http://www.spc.noaa.gov/climo/torn/fataltorn.html>]. Questions were raised almost  
5 immediately as to whether the series of extreme tornado outbreaks in 2011 could be linked to  
6 long-term climate variability. The severe weather database (SWD) from the National Oceanic  
7 and Atmospheric Administration indicates that the number of total U.S. tornadoes (i.e., from F0  
8 to F5 in the Fujita scale) during the most active tornado months of April and May (AM) has been  
9 steadily increasing since 1950 (Figure 1). However, due to numerous known deficiencies in the  
10 SWD, including improvements in tornado detection technology, increased eyewitness reports  
11 due to population increase, and changes in damage survey procedures over time, one must be  
12 cautious in attributing this secular increase in the number of U.S. tornadoes to a specific long-  
13 term climate signal (Brooks and Doswell 2001; Verbout et al. 2006).

14 In the U.S. east of the Rocky Mountains, cold and dry upper-level air from the high latitudes  
15 often converges with warm and moist lower-level air coming from the Gulf of Mexico (GoM).  
16 Due to this so-called large-scale differential advection, i.e., any vertical variation of the  
17 horizontal advection of heat and moisture that decreases the vertical stability of the air column  
18 (Whitney and Miller 1956), conditionally unstable atmosphere with high convective available  
19 potential energy is formed. The lower-level vertical wind shear associated with the upper-level  
20 westerly and lower-level southeasterly winds (i.e., wind speed increasing and wind direction  
21 changing with height) provides the spinning effect required to form a horizontal vortex tube. The  
22 axis of this horizontal vortex tube can be tilted to the vertical by updrafts and downdrafts to form  
23 an intense rotating thunderstorm known as a supercell, which is the storm type most apt to spawn

1 intense tornadoes (Lemon and Doswell 1979; Doswell and Bosart 2001). Consistently, both the  
2 moisture transport from the GoM to the U.S. and the lower-level vertical wind shear in the  
3 central and eastern U.S. are positively correlated with U.S. tornado activity in AM (Table 1).

4 The Pacific - North American (PNA) pattern in boreal winter and spring is linked to the  
5 large-scale differential advection and the lower-level vertical wind shear in the central and  
6 eastern U.S (Horel and Wallace 1981; Walalce and Gutzler 1981; Barnston and Livezey 1987).  
7 During a negative phase of the PNA, an anomalous cyclone is formed over North America that  
8 bring more cold and dry upper-level air from the high latitudes to the U.S., and an anomalous  
9 anticyclone is formed over the southeastern seaboard that increases the southwesterly wind from  
10 the GoM to the U.S., thus enhancing the Gulf-to-U.S. moisture transport. Additionally, the  
11 lower-level vertical wind shear is increased over the U.S. during a negative phase of the PNA  
12 due to the increased upper-level westerly and lower-level southeasterly. Although the PNA is a  
13 naturally occurring atmospheric phenomenon driven by intrinsic variability of the atmosphere, a  
14 La Niña in the tropical Pacific can project onto a negative phase PNA pattern (Lau and Lim  
15 1984; Straus and Shukla 2002). In addition, since the Gulf-to-U.S. moisture transport can be  
16 enhanced with a warmer GoM, the sea surface temperature (SST) anomaly in the GoM can also  
17 affect U.S. tornado activity. During the decay phase of La Niña in spring, the GoM is typically  
18 warmer than usual (Alexander and Scott 2002). Therefore, the Gulf-to-U.S. moisture transport  
19 could be increased during the decay phase of La Niña in spring due to the increased SSTs in the  
20 GoM and the strengthening of the southwesterly wind from the GoM to the U.S. Nevertheless,  
21 none of these (i.e., PNA, GoM SST, and La Nina) are highly correlated with U.S. tornado  
22 activity in AM (Table 1). Consistently, a recent study reported that the connectivity between the  
23 El Niño-Southern Oscillation (ENSO) and U.S. tornado activity is quite weak (Cook and Schafer

1 2008). Currently, seasonal forecast skill for intense U.S. tornado outbreaks, such as occurred in  
2 2011, has not been demonstrated.

3

## 4 **2. U.S. Tornado index**

5 Since intense and long-lived tornadoes are much more likely to be detected and reported even  
6 before a national network of Doppler radar was build in the 1990s, only the intense U.S.  
7 tornadoes (i.e., from F3 to F5 in the Fujita-Pearson scale) in AM during 1950-2010 from the  
8 SWD are selected and used in this study. The number of intense U.S. tornadoes is used, after  
9 detrending, as the primary diagnostic index (Figure 2b). Another tornado metric used in this  
10 study is the intense U.S. tornado-days, which is obtained by counting the number of days in  
11 which more than a threshold number of intense tornadoes occurred (Figure 2c and d), suggested  
12 by Verbout et al. (2008). The threshold number selected in this case is three and above, which  
13 roughly represents the upper 25% in the number of intense U.S. tornadoes in a given day of AM  
14 during 1950-2010. In general, the tornado count index is sensitive to big tornado outbreak days,  
15 such as April 3, 1974 during which 60 intense tornadoes occurred over the U.S. The tornado-  
16 days index is on the other hand put little weight on big tornado days. Since these two tornado  
17 indices are complementary to each other, it is beneficial to use both of these indices. The two  
18 tornado indices are further detrended and used by using a simple least squares linear regression.

19

## 20 **3. Observed relationship between Trans-Niño and U.S. tornado activity**

21 As shown in Table 1, among the long-term climate patterns considered here, only the Trans-  
22 Niño (TNI) is significantly correlated with U.S. tornado activity in AM. The TNI, which is  
23 defined as the difference in normalized SST anomalies between the Niño-1+2 ( $10^{\circ} - 0^{\circ}; 90^{\circ}W -$

1 80°W) and Niño-4 (5°N - 5°S; 160°E - 150°W) regions, represents the evolution of ENSO in the  
2 months leading up to the event and the subsequent evolution with opposite sign after the event  
3 (Trenberth and Stepaniak 2001). Given that AM is typically characterized with the development  
4 or decay phase of ENSO events, it is more likely that the tropical Pacific SST anomalies in AM  
5 are better represented by the TNI index than the conventional ENSO indices such as Niño-3.4  
6 (5°N - 5°S; 170°W - 120°W) or Niño-3 (5°N - 5°S; 150°W-90°W). Nevertheless, it is not clear  
7 why U.S. tornado activity in AM is more strongly correlated with the TNI index than with other  
8 ENSO indices.

9 It is noted that the historical time series for the number of intense (from F3 to F5 in the  
10 Fujita-Pearson scale) tornadoes is characterized by intense tornado outbreak years, such as 1974,  
11 1965 and 1957, embedded amongst much weaker amplitude fluctuations (Figure 2a and b). Since  
12 the majority of tornado-related fatalities occur during those extreme outbreak years, here we  
13 focus our attention to those extreme years and associated climate signals. Therefore, we ranked  
14 the years from 1950 to 2010 (61 years in total) based on the number of intense U.S. tornadoes in  
15 AM.

16 The top ten extreme tornado outbreak years are characterized by an anomalous upper-level  
17 cyclone over North America that advects more cold and dry air to the U.S. (Figure 3a), increased  
18 Gulf-to-U.S. moisture transport (Figure 3b) and increased lower-level vertical wind shear over  
19 the central and eastern U.S. (Figure 3c), whereas the bottom ten years are associated with an  
20 anomalous upper-level anticyclone over North America (Figure 3d), decreased Gulf-to-U.S.  
21 moisture transport (Figure 3e) and decreased lower-level vertical wind shear over the central and  
22 eastern U.S. (Figure 3f). Note that if the tornado ranking is redone based on the intense U.S

1 tornado-days in AM, 1998 in the top ten list is replaced by 1960, but other top nine years remain  
2 in the top ten (not shown).

3 As in the top ten extreme tornado outbreak years, the top ten positive TNI years are also  
4 characterized by an anomalous upper-level cyclone over North America (Figure 4a), increased  
5 Gulf-to-U.S. moisture transport (Figure 4b) and increased lower-level vertical wind shear over  
6 the central and eastern U.S. (Figure 4c). Consistently, among the top ten extreme tornado  
7 outbreak years, seven years including the top three are identified with a positive phase (i.e.,  
8 within the upper quartile) TNI index (i.e., normalized SST anomalies are larger in the Niño-1+2  
9 than in Niño-4 region) (Table 2). Five out of those seven years are characterized by a La Niña  
10 transitioning to a different phase or persisting beyond AM (1957, 1965, 1974, 1999, and 2008)  
11 and the other two with an El Niño transitioning to either a La Nina or neutral phase (1983 and  
12 1998). In the composite SST anomalies for those five positive phase TNI years transitioning  
13 from a La Niña, the central tropical Pacific (CP) and the eastern tropical Pacific (EP) are  
14 characterized by cooling and warming, respectively (Figure 5a).

15 On the other hand, among the bottom ten years (Table 3), only one year is identified with a  
16 positive phase TNI, and the other nine years are with a neutral phase TNI (i.e., between the lower  
17 and upper quartiles), suggesting that a negative phase of the TNI neither decreases nor increases  
18 the number of intense U.S. tornadoes in AM. Interestingly, four years among the bottom ten  
19 years are identified with a La Niña transitioning to a different phase or persisting beyond AM  
20 (1950, 1951, 1955 and 2001), and four are identified with an El Niño transitioning to a different  
21 phase or persisting beyond AM (1958, 1987, 1988 and 1992). The composite SST anomaly  
22 pattern for the four years of the bottom ten years with a La Niña transitioning is that of a typical  
23 La Niña with the SST anomalies in the Niño-4 and Niño-1+2 being both strongly negative (i.e.,

1 neutral phase TNI) (Figure 5b). Similarly, the composite SST anomaly pattern for the four years  
2 in the bottom ten years with an El Niño transitioning is that of a typical El Niño with the SST  
3 anomalies in the Niño-4 and Niño-1+2 being both strongly positive (i.e., neutral phase TNI)  
4 (Figure 5c).

5 In summary, observations seem to indicate that a positive phase of the TNI (i.e., normalized  
6 SST anomalies are larger in the Niño-1+2 than in Niño-4 region) is linked to increased U.S.  
7 tornado activity in AM, whereas either La Niñas and El Niños with a neutral phase TNI (i.e., the  
8 SST anomalies in the Niño-1+2 region are as strong and the same sign as the SST anomalies in  
9 the Niño-4) are not linked to increased U.S. tornado activity in AM.

10

#### 11 **4. Model Experiments**

12 To explore the potential link between the three tropical Pacific SST anomaly patterns  
13 identified in the previous section (Figure 3) and the number of intense U.S. tornadoes in AM, a  
14 series of AGCM experiments are performed by using version 3.1 of the NCAR community  
15 atmospheric model coupled to a slab mixed layer ocean model (CAM3). The model is a global  
16 spectral model with a triangular spectral truncation of the spherical harmonics at zonal wave  
17 number 42. It is vertically divided into 26 hybrid sigma-pressure layers. Model experiments are  
18 performed by prescribing various composite evolutions of SSTs in the tropical Pacific region  
19 (15°S–15°N; 120°E-coast of the Americas) while predicting the SSTs outside the tropical Pacific  
20 using the slab ocean model. To prevent discontinuity of SST around the edges of the forcing  
21 region, the model SSTs of three grid points centered at the boundary are determined by  
22 combining the simulated and prescribed SSTs. Each ensemble consists of ten model integrations  
23 that are initialized with slightly different conditions to represent intrinsic atmospheric variability.



1 The same methodology was previously used for studying ENSO teleconnection to the tropical  
2 North Atlantic region (Lee et al. 2008).

3 Four sets of ensemble runs are performed (Table 4). In the first experiment (EXP\_CLM), the  
4 SSTs in the tropical Pacific region are prescribed with climatological SSTs. In the second  
5 experiment (EXP\_TNI), the composite SSTs of the positive phase TNI years identified among  
6 the ten most active U.S. tornado years are prescribed in the tropical Pacific region. Note that only  
7 the five positive TNI years transitioning from a La Niña (1957, 1965, 1974, 1999, and 2008) are  
8 considered here because the other two positive TNI years are transitioning from an El Niño  
9 (1983 and 1998) and thus tend to cancel the tropical SST anomalies of the other five. In the next  
10 two experiments, the SSTs in the tropical Pacific region are prescribed with the composite SSTs  
11 of the four years in the bottom ten years with a La Niña transitioning (1950, 1951, 1955 and  
12 2001) for EXP\_LAN, and the four years in the bottom ten years with an El Niño transitioning  
13 (1958, 1987, 1988 and 1992) for EXP\_ELN.

14

## 15 **5. Simulated impact of TNI on tornadic environments**

16 In EXP\_TNI (Figure 6), an anomalous upper-level cyclone is formed over North America  
17 that brings more cold and dry air to the U.S., and both the Gulf-to-U.S. moisture transport and  
18 the lower-level vertical wind shear over the central and eastern U.S. are increased, all of which  
19 are large-scale atmospheric conditions conducive to intense tornado outbreaks over the U.S.

20 In EXP\_ELN (Figure 7a, b and c), on the other hand, the Gulf-to-U.S. moisture transport is  
21 neither increased nor decreased. The lower-level vertical wind shear is slightly decreased over  
22 the central and eastern U.S. mainly due to a weak anomalous upper-level anticyclone formed  
23 over North America. In EXP\_LAN (Figure 7d, e and f), a relatively weak anomalous upper-level

1 cyclone is formed, and thus the lower-level vertical wind shear is slightly increased. However,  
2 the Gulf-to-U.S. moisture is not increased.

3 Therefore, these model results support the hypothesis that a positive phase of the TNI with  
4 cooling in CP and warming in EP enhances the large-scale differential advection in the central  
5 and eastern U.S. and increases the lower-level vertical wind shear therein, thus providing large-  
6 scale atmospheric conditions conducive to intense tornado outbreaks over the U.S. However, the  
7 model results do not show favorable large-scale atmospheric conditions in the central and eastern  
8 U.S. under La Niña and El Niño conditions as long as the SST anomalies in EP are as strong and  
9 the same sign as the SST anomalies in CP.

10

## 11 **6. CP- versus EP-forced teleconnection**

12 The model results strongly suggest that cooling in CP and warming in EP may have a  
13 constructive influence on the teleconnection pattern that strengthens the large-scale differential  
14 advection and lower-level vertical wind shear over the central and eastern U.S. To better  
15 understand how the real atmosphere with moist diabatic processes responds to CP cooling and  
16 EP warming, two sets of additional model experiments (EXP\_CPC and EXP\_EPW) are  
17 performed (Table 4). These two experiments are basically identical to EXP\_TNI except that the  
18 composite SSTs of the positive phase TNI years are prescribed only in the western and central  
19 tropical Pacific region (15°S–15°N; 120°E - 110°W) for EXP\_CPC and only in the eastern  
20 tropical Pacific region (15°S–15°N; 110°W-coast of the Americas) for EXP\_EPW.

21 In EXP\_CPC (Figure 8a, b and c), the teleconnection pattern emanating from the tropical  
22 Pacific consists of an anticyclone over the Aleutian Low in the North Pacific, a cyclone over  
23 North America, and an anticyclone over the southeastern U.S. extending to meso-Americas,

1 consistent with a negative phase PNA-like pattern (Figure 8a). As expected from the anomalous  
2 anticyclonic circulation over the southeastern U.S. and meso-America, the Gulf-to-U.S. moisture  
3 transport is increased in EXP\_CPC (Figure 8b). The lower-level vertical wind shear is increased  
4 over the central and eastern U.S. due to the strengthening of the upper-level westerly and lower-  
5 level southeasterly winds (Figure 8c).

6 Surprisingly, the Rossby wave train forced by warming in EP (EXP\_EPW) is very similar to  
7 that in EXP\_CPC (Figure 8d). Consistently, both the Gulf-to-U.S. moisture transport and the  
8 lower-level vertical wind shear over the central and eastern U.S. are also increased in EXP\_EPW  
9 as in EXP\_CPC and EXP\_TNI (Figure 8e and f). A question arises as to why the teleconnection  
10 pattern forced by warming in EP is virtually the same as that forced by cooling in CP. It appears  
11 that the Rossby wave train in EXP\_EPW is not directly forced from EP. In EXP\_EPW,  
12 convection is increased locally in EP, but it is decreased in CP as in EXP\_CPC (Figure 9c). This  
13 suggests that increased convection in EP associated with the increased local SSTs suppresses  
14 convection in CP that in turn forces a negative phase PNA-like pattern. Therefore, these model  
15 results confirm that cooling in CP and warming in EP do have constructive influence on the  
16 teleconnection pattern that strengthens the large-scale differential advection and lower-level  
17 vertical wind shear over the central and eastern U.S. The model results also suggest that cooling  
18 in CP with neutral SST anomalies in EP or warming in EP with neutral SST anomalies in CP can  
19 strengthen the large-scale differential advection and lower-level vertical wind shear over the  
20 central and eastern U.S.

21 An apparently important question is why warming in EP does not directly excite a Rossby  
22 wave train to the high-latitudes. As shown in earlier theoretical studies, the vertical background  
23 wind shear is one of the two critical factors required for tropical heating to radiate barotropic

1 teleconnections to the high-latitudes (e.g., Lee et al. 2009). In both observations and EXP\_CLM,  
2 the background vertical wind shear between 200 and 850 hPa in AM is largest in the central  
3 tropical North Pacific and smallest in EP and the western tropical Pacific (WP), providing an  
4 explanation as to why the Rossby wave train in EXP\_EPW is not directly forced in EP (Figure  
5 10).

6

## 7 **7. Implications for a seasonal outlook for extreme U.S. tornado outbreaks**

8 The conclusion so far is that a positive phase of the TNI, characterized by cooling in CP and  
9 warming in EP, strengthens the large-scale differential advection and lower-level vertical wind  
10 shear in the central and eastern U.S., and thus provides favorable large-scale atmospheric  
11 conditions for major tornado outbreaks over the U.S. However, the TNI explains only up to 10%  
12 of the total variance in the number of intense U.S. tornadoes in AM. This suggests that intrinsic  
13 variability in the atmosphere may overwhelm the TNI-teleconnection pattern over North  
14 America as discussed in earlier studies for El Niño-teleconnection patterns in the Pacific–North  
15 American region (e.g., Hoerling and Kumar 1997). In other words, the predictability of U.S.  
16 tornado activity, which can be defined as a ratio of the climate signal (the TNI index in this case)  
17 relative to the climate noise, is low.

18 Nevertheless, seven of the ten most extreme tornado outbreak years during 1950-2010  
19 including the top three years are characterized by a strongly positive phase of the TNI (Table 2).  
20 A practical implication of this result is that a seasonal outlook for extreme U.S. tornado  
21 outbreaks may be achievable if a seasonal forecasting system has significant skill in predicating  
22 the TNI and associated teleconnections to the U.S. Obviously, before we can achieve such a  
23 goal, there remain many crucial scientific questions to be addressed to refine the predictive skill

1 provided by the TNI and to explore other long-term climate signals that can provide additional  
2 predictability in seasonal and longer time scales.

3

#### 4 **8. U.S. Tornado Outbreaks in 2011**

5 A positive phase of the TNI prevailed during AM of 2011 with cooling in CP and warming  
6 EP (Figure 11). An important question is whether the series of extreme U.S. tornado outbreaks  
7 during AM of 2011 can be attributed to this positive phase of the TNI. During AM of 2011, an  
8 anomalous upper-level cyclone was formed over the northern U.S. and southern Canada (Figure  
9 12a), the Gulf-to-US moisture was greatly increased (Figure 12b), and the lower-level vertical  
10 wind shear was increased over the central U.S. (Figure 12c), all indicating the coherent  
11 teleconnection response to a positive phase of the TNI. To confirm this, a set of model  
12 experiments (EXP\_011) is performed by prescribing the SSTs for 2010 - 2011 in the tropical  
13 Pacific region while predicting the SSTs outside the tropical Pacific using the slab ocean model  
14 (Table 4). As summarized in Figure 13, the model results are consistent with the observations,  
15 although the anomalous Gulf-to-US moisture transport is weaker in the model experiment.

16 A distinctive feature in the 2011 TNI event is warming in WP (Figure 11). Further  
17 experiments (Table 4) suggest that the warming in WP indirectly suppresses convection in CP,  
18 and thus works constructively with the cooling in CP to force a strong and persistent negative  
19 phase PNA-like pattern (Figure 14 and 15). Thus, it is highly likely that the 2011 positive phase  
20 TNI event did contribute to the U.S. tornado outbreak in AM of 2011 by enhancing the  
21 differential advection and lower-level vertical wind shear in the central and eastern U.S.

22

#### 23 **9. Discussions**

1 One of the caveats in this study, as in any tornado related climate research, is an artificial  
2 inhomogeneity in the tornado database. Eyewitness reports are important sources for tornado  
3 count, which can be affected by population growth and migration. Additionally, tornado rating is  
4 largely based on structural damage - wind speed relationship, which can change with time and  
5 case-by-case because every particular tornado - structure interaction is different in detail. For  
6 these and other reasons, the historical time series of the tornado database cannot be completely  
7 objective or consistent over time (Doswell et al. 2009). In this study, only the intense U.S.  
8 tornadoes (F3 - F5) are selected and used since intense and long-lived tornadoes are less likely to  
9 be affected by, although not completely free from, such issues in the tornado database. An  
10 alternative approach is to develop and use a proxy tornado database, which can be derived from  
11 tornadic environmental conditions in atmospheric reanalysis products. Results from a recent  
12 study that used such an approach were promising (Brooks et al. 2003).

13

14 **Acknowledgments.** We would like to thank Herold Brooks, Charles Doswell, Brian Mapes and  
15 Gregory Carbin for their thoughtful comments and suggestions. This study was motivated and  
16 benefited from interactions with scientists at NOAA ESRL, GFDL, CPC, NCDC and AOML. In  
17 particular, we wish to thank Wayne Higgins, Tom Karl and Marty Hoerling for initiating and  
18 leading discussions that motivated this study. This work was supported by grants from the  
19 National Oceanic and Atmospheric Administration's Climate Program Office and by grants from  
20 the National Science Foundation.

21

22

## REFERENCES

- 1 Alexander, M., and J. Scott, 2002: The influence of ENSO on air-sea interaction in the Atlantic.  
2 *Geophys. Res. Lett.*, **29**, 1701, doi:10.1029/2001GL014347.
- 3 Barnston A. G., and R. E. Livezey, 1987: Classification, seasonality, and persistence of low-  
4 frequency atmospheric circulation patterns. *Mon. Weather Rev.*, **115**, 1083–1126.
- 5 Brooks, H. E., C. A. Doswell III, 2001: Some aspects of the international climatology of  
6 tornadoes by damage classification. *Atmos. Res.* **56**, 191– 201.
- 7 Brooks, H. E., J. W. Lee, and J. P. Cravenc, 2003: The spatial distribution of severe  
8 thunderstorm and tornado environments from global reanalysis data, *Atmos. Res.*, **67-68**, 73-  
9 94.
- 10 Cook, A. R., J. T. Schaefer, 2008: The relation of El Niño–Southern Oscillation (ENSO) to  
11 winter tornado outbreaks, *Mon. Wea. Rev.*, **136**, 3121–3137.
- 12 Doswell III, C. A., L. F. Bosart, 2001: Extratropical synoptic-scale processes and severe  
13 convection. Severe Convection Storms. *Meteor. Monogr.* **28**, Amer. Meteor. Soc. 27-69.
- 14 Doswell III, C. A., H. E. Brooks, and N. Dotzek, 2009: On the implementation of the Enhanced  
15 Fujita Scale in the USA. *Atmos. Res.*, **93**, 554-563, doi:10.1016/j.atmosres.2008.11.003.
- 16 Hoerling, M. P., and A. Kumar, 1997: Why do North American climate anomalies differ from  
17 one El Niño event to another?, *Geophys. Res. Lett.*, **24**, 1059-1062.
- 18 Horel, J. D., and J. M. Wallace, 1981: Planetary-scale atmospheric phenomena associated with  
19 the Southern Oscillation. *Mon. Wea. Rev.* **109**, 813–829.
- 20 Lau, K.-M., and H. Lim, 1984: On the dynamics of equatorial forcing of climate teleconnections.  
21 *J. Atmos. Sci.*, **41**, 161–176.
- 22 Lee, S.-K., D. B. Enfield, and C. Wang, 2008: Why do some El Ninos have no impact on tropical  
23 North Atlantic SST? *Geophys. Res. Lett.*, **35**, L16705, doi:10.1029/2008GL034734.

- 1 Lee, S.-K., C. Wang, and B. E. Mapes, 2009: A simple atmospheric model of the local and  
2 teleconnection responses to tropical heating anomalies. *J. Clim.*, **22**, 272-284.
- 3 Lemon, L. R., and C. A. Doswell III, 1979: Severe thunderstorm evolution and mesocyclone  
4 structure as related to tornadogenesis. *Mon. Wea. Rev.* **107**, 1184–1197.
- 5 Straus, D. M., J. Shukla, 2002: Does ENSO force the PNA?, *J. Clim.*, **15**, 2340–2358.
- 6 Trenberth, K. E., and D. P. Stepaniak, 2001: Indices of El Niño evolution, *J. Clim.*, **14**, 1697–  
7 1701.
- 8 Verbout, S. M., H. E. Brooks, L. M. Leslie, and D. M. Schultz, 2006: Evolution of the U.S.  
9 tornado database: 1954-2003. *Wea. Forecasting* **21**, 86-93.
- 10 Wallace, J. M., and D. S. Gutzler, 1981: Teleconnections in the geopotential height field during  
11 the Northern Hemisphere winter. *Mon. Wea. Rev.* **109**, 784–804.
- 12 Whitney Jr., L. F., and J. E. Miller, 1956: Destabilization by differential advection in the tornado  
13 situation 8 June 1953. *Bull. Amer. Meteor. Soc.* **37**, 224–229.



**Table 1.** Correlation coefficients of various long-term climate patterns in December-February (DJF), February-April (FMA), and April and May (AM) with the number of intense tornadoes in AM during 1950-2010. The values in parenthesis are those with the intense U.S. tornado-days in AM during 1950-2010. All indices including the tornado index are detrended using a simple least squares linear regression. The SWD, ERSST3, and NCEP-NCAR reanalysis are used to obtain the long-term climate indices used in this table. Correlation coefficients above the 95% significance are in bold<sup>a</sup>.

Index	DJF	FMA	AM
Gulf-to-U.S. moisture transport	0.08 ( 0.05)	0.20 ( 0.14)	<b>0.40 ( 0.36)</b>
Lower-level vertical wind shear	0.06 ( 0.04)	0.15 ( <b>0.25</b> )	<b>0.34 ( 0.30)</b>
GoM SST	0.15 ( 0.15)	0.21 ( 0.16)	0.20 ( 0.19)
Niño-4	-0.22 (-0.19)	-0.20 (-0.18)	-0.19 (-0.18)
Niño-3.4	-0.13 (-0.11)	-0.13 (-0.12)	-0.11 (-0.11)
Niño-1+2	0.02 ( 0.03)	0.11 ( 0.11)	0.15 ( 0.13)
TNI	<b>0.28 ( 0.26)</b>	<b>0.29 ( 0.28)</b>	<b>0.33 ( 0.29)</b>
PNA	-0.05 (-0.02)	-0.10 (-0.06)	-0.20 (-0.16)
PDO	-0.12 (-0.09)	-0.10 (-0.11)	-0.14 (-0.20)
NAO	-0.01 (-0.07)	-0.10 (-0.14)	-0.18 (-0.18)

<sup>a</sup>The Gulf-to-U.S. meridional moisture transport is obtained by averaging the vertically integrated moisture transport in the region of 25°N - 35°N and 100°W - 90°W. The lower-level (500 hPa – 925 hPa) vertical wind shear is averaged over the region of 30°N – 40°N and 100°W – 80°W. The North Atlantic Oscillation (NAO) index and the Pacific - North American (PNA) pattern are defined as the first and second leading modes of Rotated Empirical Orthogonal Function (REOF) analysis of monthly mean geopotential height at 500 hPa, respectively. The Pacific Decadal Oscillation (PDO) is the leading principal component of monthly SST anomalies in the North Pacific Ocean north of 20°N.

**Table 2.** The total of 61 years from 1950 to 2010 are ranked based on the detrended number of intense U.S. tornadoes in AM. The top ten extreme U.S. tornado outbreak years are listed with ENSO phase in spring and TNI index in AM for each year. Strongly positive (i.e., the upper quartile) and negative (i.e., the lower quartile) TNI index values are in bold and italic, respectively.

Ranking	Year	ENSO phase in spring	TNI index (detrended)
1	1974	La Niña persists	<b>1.30 ( 1.48)</b>
2	1965	La Niña transitions to El Niño	<b>1.39 ( 1.54)</b>
3	1957	La Niña transitions to El Niño	<b>0.57 ( 0.69)</b>
4	1982	El Niño develops	<i>-1.11 (-0.89)</i>
5	1973	El Niño transitions to La Niña	<i>-0.42 (-0.24)</i>
6	1999	La Niña persists	<b>0.47 ( 0.75)</b>
7	1983	El Niño decays	<b>1.86 ( 2.08)</b>
8	2003	El Niño decays	<i>-1.24 (-0.94)</i>
9	2008	La Niña decays	<b>1.41 ( 1.73)</b>
10	1998	El Niño transitions to La Niña	<b>1.69 ( 1.97)</b>

**Table 3.** The total of 61 years from 1950 to 2010 are ranked based on the detrended number of intense U.S. tornadoes in AM. The bottom ten years are listed with ENSO phase in spring and TNI index in AM for each year. Strongly positive (i.e., the upper quartile) and negative (i.e., the lower quartile) TNI index values are in bold and italic, respectively.

Ranking	Year	ENSO phase in spring	TNI index (detrended)
52	1958	El Niño decays	-0.61 (-0.49)
53	1955	La Niña persists	-0.27 (-0.16)
54	2001	La Niña decays	0.21 ( 0.50)
55	1986	El Niño develops	-0.39 (-0.16)
56	1988	El Niño transitions to La Niña	-0.37 (-0.13)
57	1987	El Niño persists	0.10 ( 0.34)
58	1992	El Niño decays	0.21 ( 0.47)
59	1952	Neutral	-0.67 (-0.57)
60	1951	La Niña transitions to El Niño	-0.31 (-0.22)
61	1950	La Niña persists	<b>0.77 ( 0.86)</b>

**Table 4.** Prescribed SSTs in the tropical Pacific region for each model experiment. All model experiments are initiated from April of the prior year to December of the modeling year. For instance, in EXP\_TNI, the model is integrated for 21 months starting in April using the composite April SSTs of 1956, 1964, 1973, 1998, and 2007.

Experiments	Prescribed SSTs in the tropical Pacific region
EXP_CLM	Climatological SSTs are prescribed in the tropical Pacific region (15°S–15°N; 120°E-coast of the Americas).
EXP_TNI	Composite SSTs of the five positive phase TNI years transiting from a La Niña identified among the ten most active U.S. tornado years (1957, 1965, 1974, 1999, and 2008) are prescribed in the tropical Pacific region.
EXP_LAN	Composite SSTs of the four years with a La Niña transitioning (1950, 1951, 1955 and 2001) identified among the ten least active U.S. tornado years are prescribed in the tropical Pacific region.
EXP_ELN	Composite SSTs of the four years with an El Niño transitioning (1958, 1987, 1988 and 1992) identified among the ten least active U.S. tornado years are prescribed in the tropical Pacific region
EXP_CPC	Same as EXP_TNI except that the composite SSTs are prescribed only in the western and central tropical Pacific region (15°S–15°N; 120°E - 110°W).
EXP_EPW	Same as EXP_TNI except that the composite SSTs are prescribed only in the eastern tropical Pacific region (15°S–15°N; 110°W-coast of the Americas).
EXP_011	SSTs for 2010-2011 are prescribed in the tropical Pacific region.
EXP_WPW	Same as EXP_011 except that the SSTs for 2010-2011 are prescribed only in the western Pacific region (15°S–15°N; 120°E - 180°).

SWD: Number of All U.S. Tornadoes (APR–MAY)

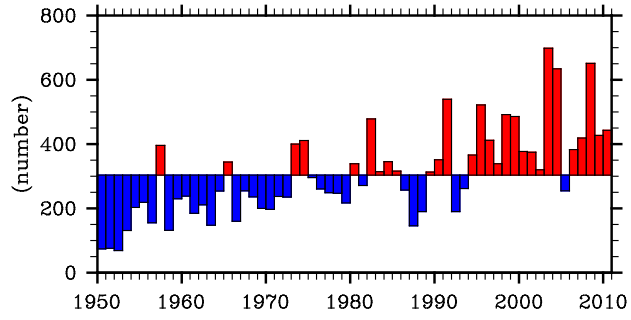


**Figure 1.** The number of all (F0 – F5) U.S. tornadoes for the most active tornado months of April and May (AM) during 1950-2010 obtained from SWD.

SWD: U.S. Tornadoes (APR–MAY)

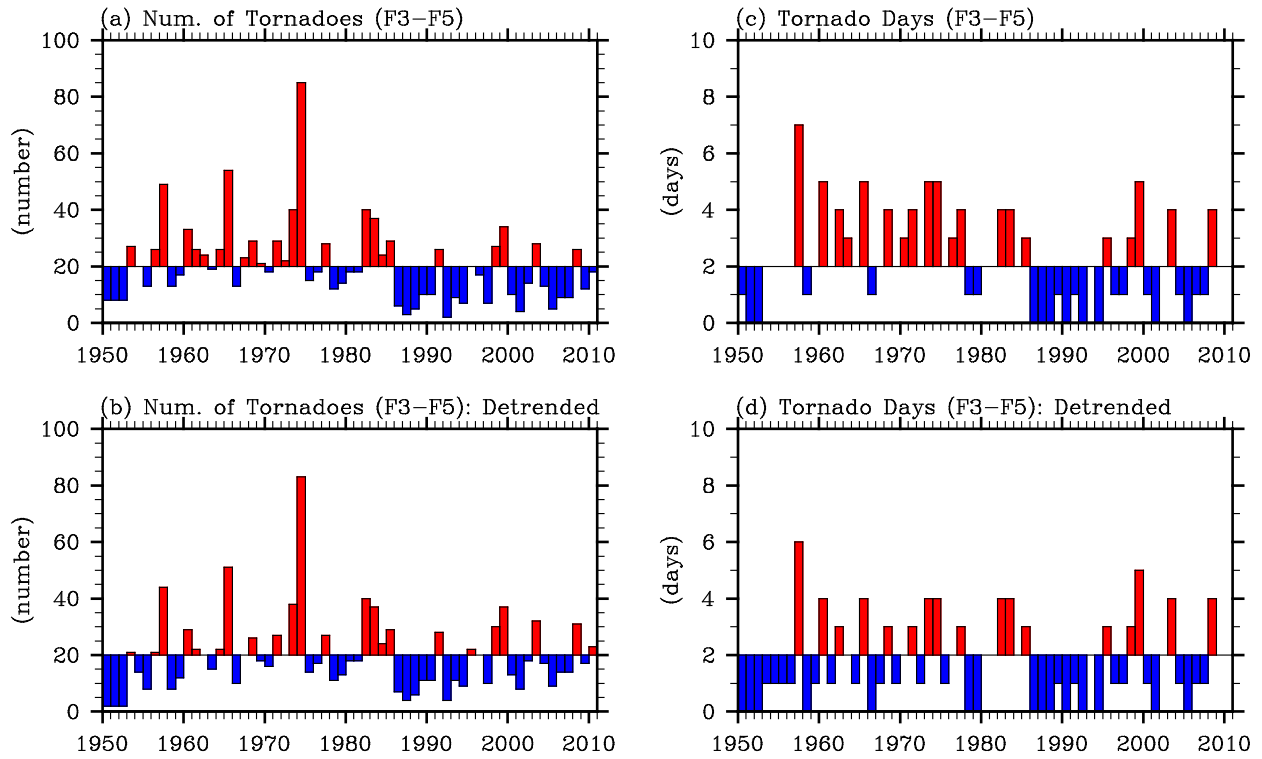


**Figure 2.** (a) The number of intense (F3 – F5) U.S. tornadoes and (c) the intense tornado-days for the most active tornado months of April and May (AM) during 1950-2010 obtained from SWD. The intense U.S. tornado-days is obtained by counting the number of days in which more than three intense tornadoes occurred. The detrended number of intense tornadoes and the detrended intense tornado-days are shown in (b) and (d), respectively.

NCEP-NCAR Reanalysis: Key Atmospheric Conditions during Active and Inactive Years (APR-MAY)

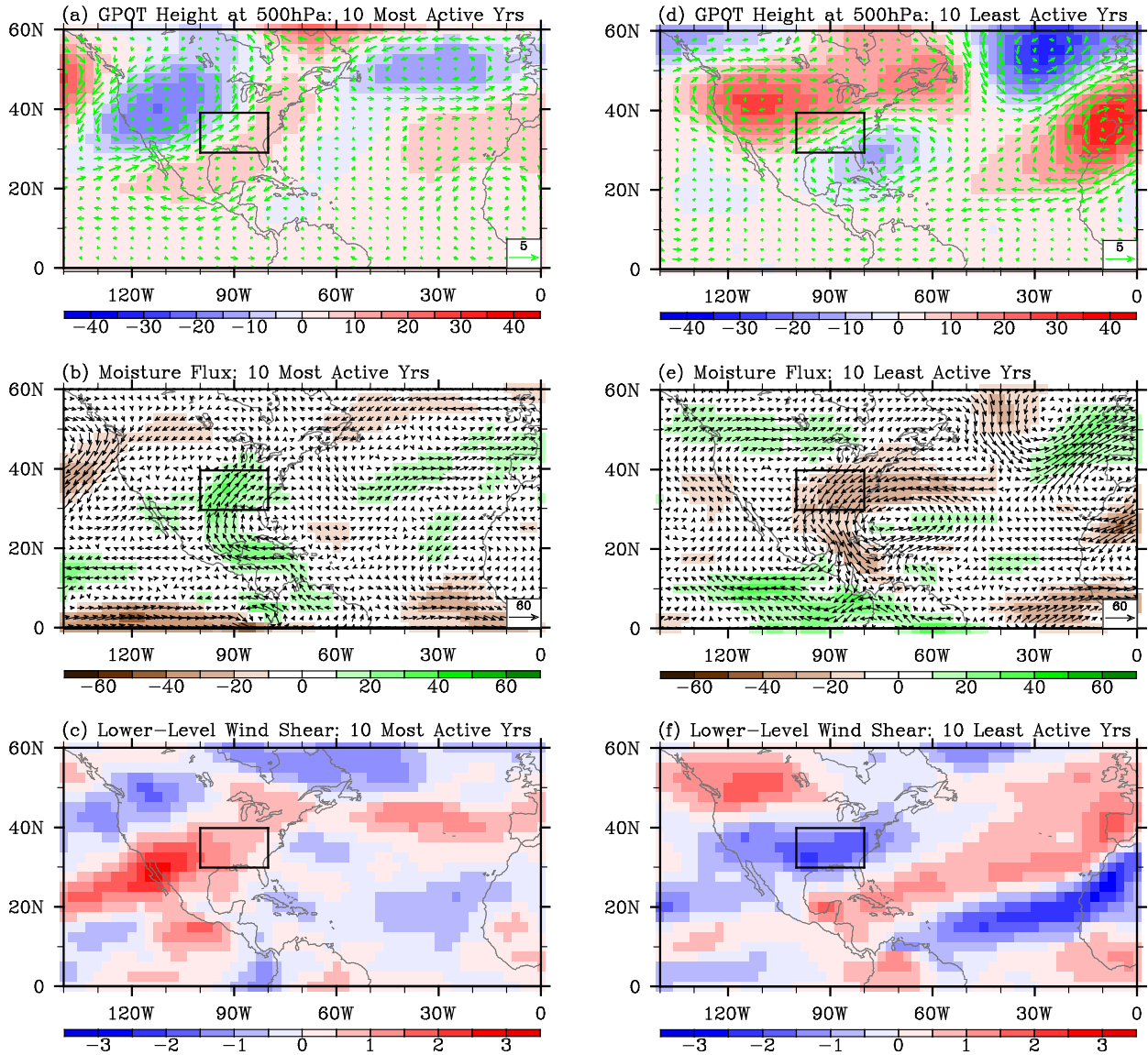


**Figure 3.** Anomalous geopotential height and wind at 500 hPa, moisture transport and lower-level (500 hPa – 925 hPa) vertical wind shear for the ten most active U.S. tornado years (a, b and c) and the ten least active U.S. tornado years (d, e and f) in AM during 1950-2010 obtained from NCEP-NCAR reanalysis. The units are  $\text{kg m}^{-1}\text{sec}^{-1}$  for moisture transport, m for geopotential height, and  $\text{m s}^{-1}$  for wind and wind shear. The small box in (a) - (f) indicates the central and eastern U.S. region frequently affected by intense tornadoes.

NCEP-NCAR Reanalysis: Pos. TNI Years (APR-MAY)

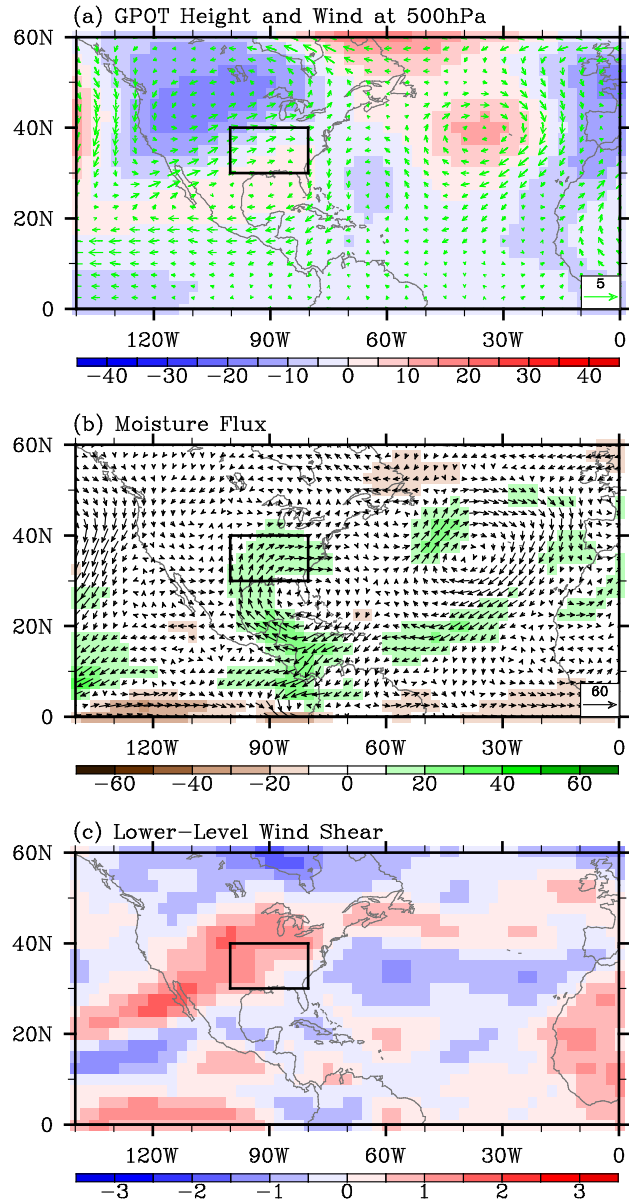


**Figure 4.** Anomalous (a) geopotential height and wind at 500 hPa, (b) moisture transport and (c) lower-level (500 hPa – 925 hPa) vertical wind shear for the top ten positive TNI years in AM during 1950-2010 obtained from NCEP-NCAR reanalysis. The units are  $\text{kg m}^{-1}\text{sec}^{-1}$  for moisture transport, m for geopotential height, and  $\text{m s}^{-1}$  for wind and wind shear. The small box in (a) - (c) indicates the central and eastern U.S. region frequently affected by intense tornadoes.



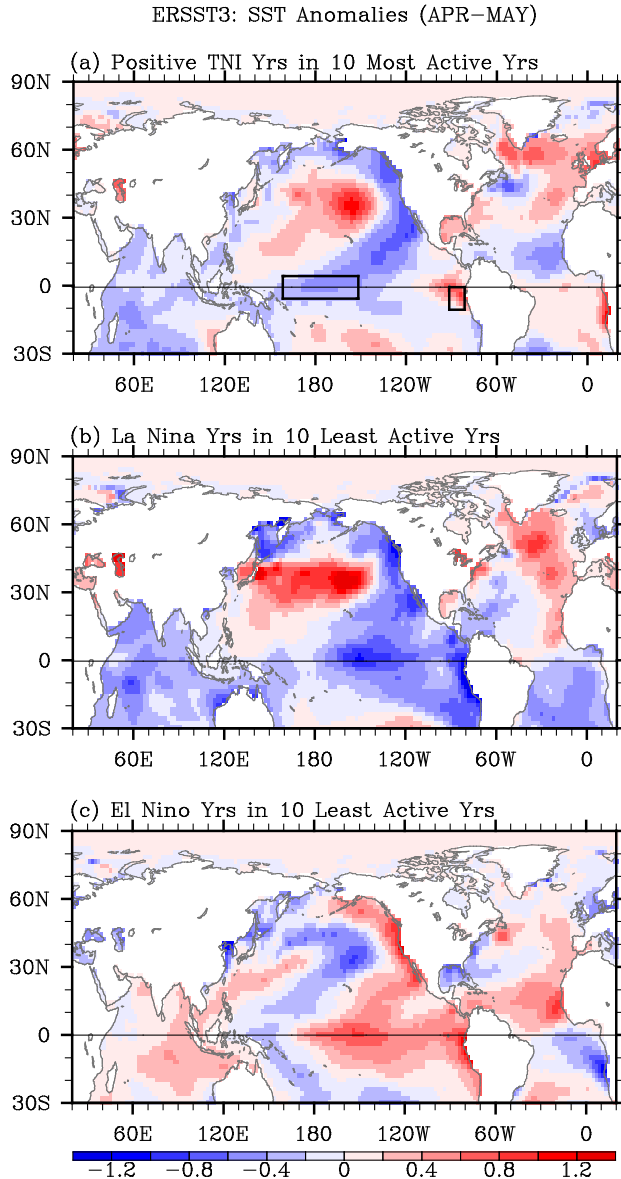


**Figure 5.** Composite SST anomalies in AM, obtained from ERSST3, for (a) the five positive TNI years transitioning from a La Niña identified among the ten most active U.S. tornado years in AM during 1950-2010, and for (b) the four years with a La Niña transitioning and (c) the four years with an El Niño transitioning identified among the ten least active U.S. tornado years in AM during 1950-2010. Thick black rectangles in (a) indicate the Niño-4 ( $5^{\circ}\text{N} - 5^{\circ}\text{S}$ ;  $160^{\circ}\text{E} - 150^{\circ}\text{W}$ ) and Niño-1+2 ( $10^{\circ}\text{S} - 0^{\circ}$ ;  $90^{\circ}\text{W} - 80^{\circ}\text{W}$ ) regions.

CAM3: EXP\_TNI - EXP\_CLM (APR-MAY)

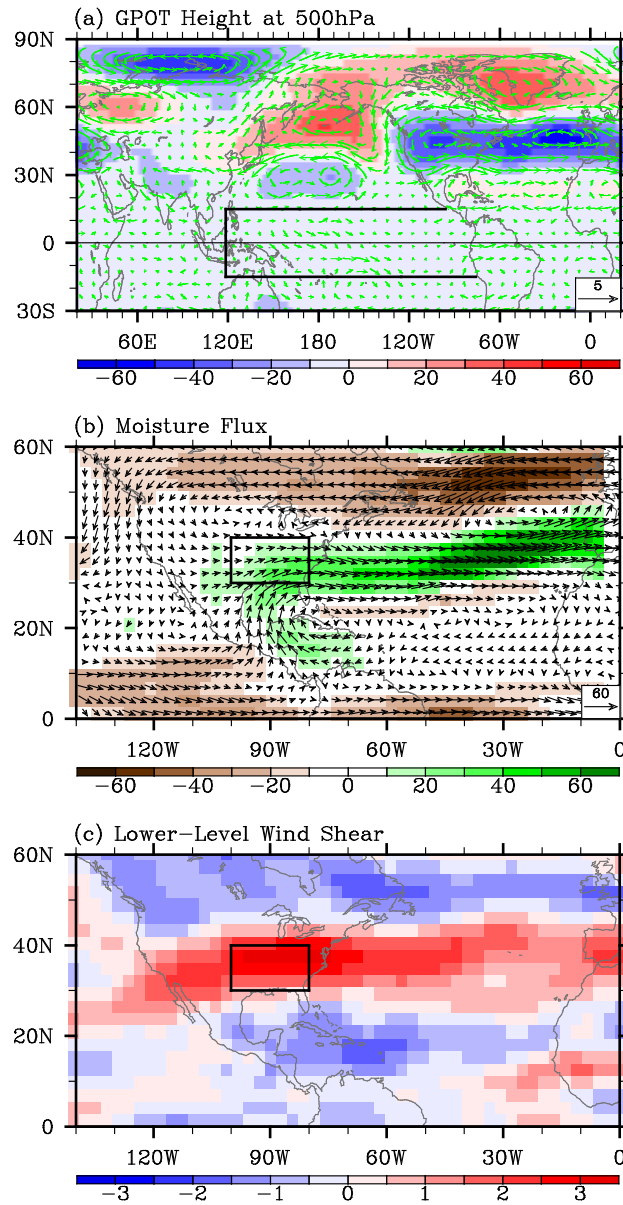


**Figure 6.** Simulated anomalous (a) geopotential height and wind at 500 hPa, (b) moisture transport and (c) lower-level (500 hPa - 925 hPa) vertical wind shear in AM obtained from EXP\_TNI - EXP\_CLM. The units are  $\text{kg m}^{-1} \text{sec}^{-1}$  for moisture transport, m for geopotential height, and  $\text{m s}^{-1}$  for wind and wind shear. Thick black lines in (a) indicate the tropical Pacific region where the model SSTs are prescribed. The small box in (b) and (c) indicates the central and eastern U.S. region frequently affected by intense tornadoes.

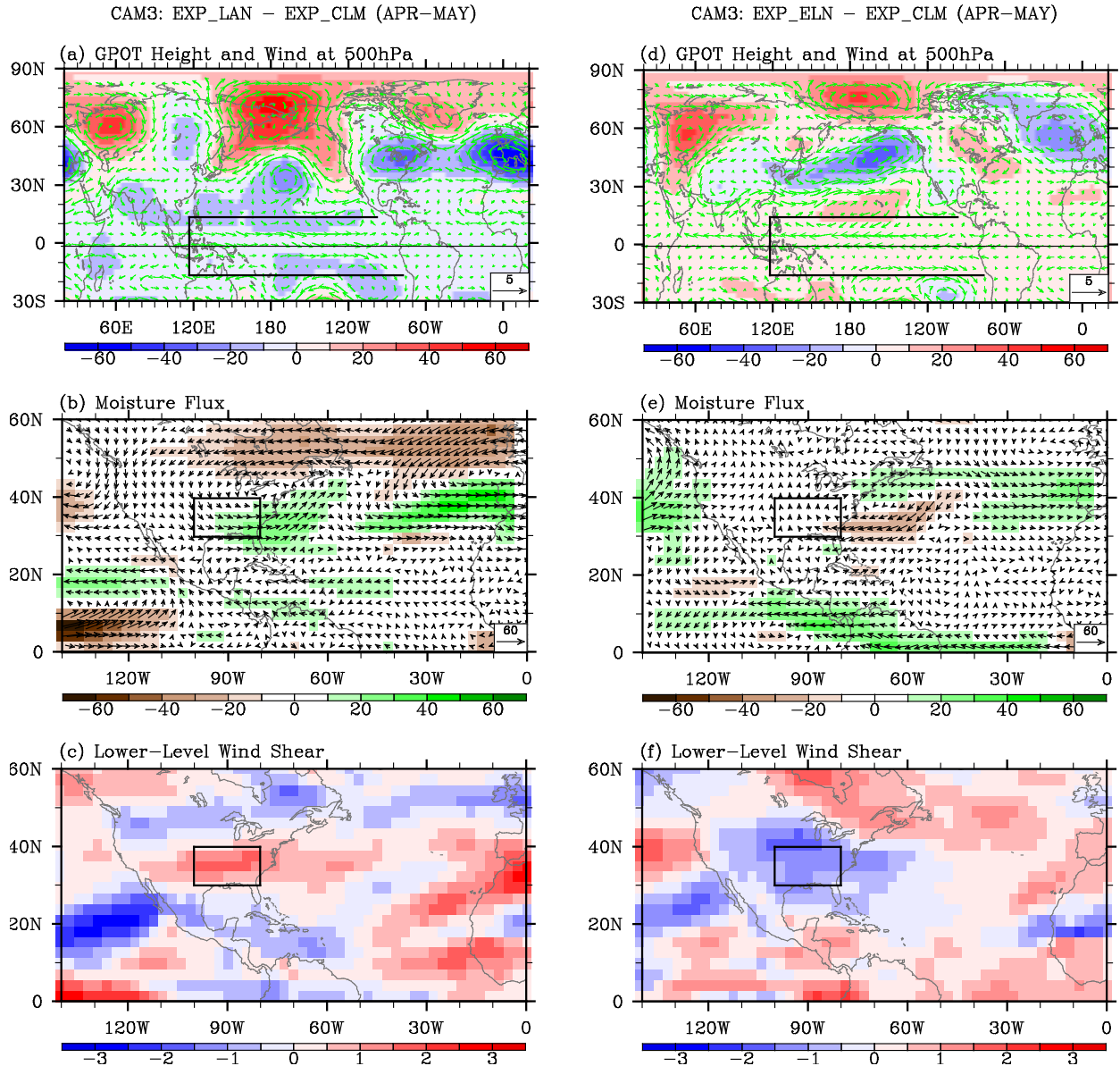


**Figure 7.** Simulated anomalous geopotential height and wind at 500, moisture transport and (c) lower-level (500 hPa – 925 hPa) vertical wind shear in AM obtained from EXP\_LAN – EXP\_CLM (a, b and c) and EXP\_ELN – EXP\_CLM (d, e and f). The unit is  $\text{kg m}^{-1} \text{sec}^{-1}$  for moisture transport, m for geopotential height, and  $\text{m s}^{-1}$  for wind and wind shear. Thick black lines in (a) and (d) indicate the tropical Pacific region where the model SSTs are prescribed. The small box in (b), (c), (e) and (f) indicates the central and eastern U.S. region frequently affected by intense tornadoes.

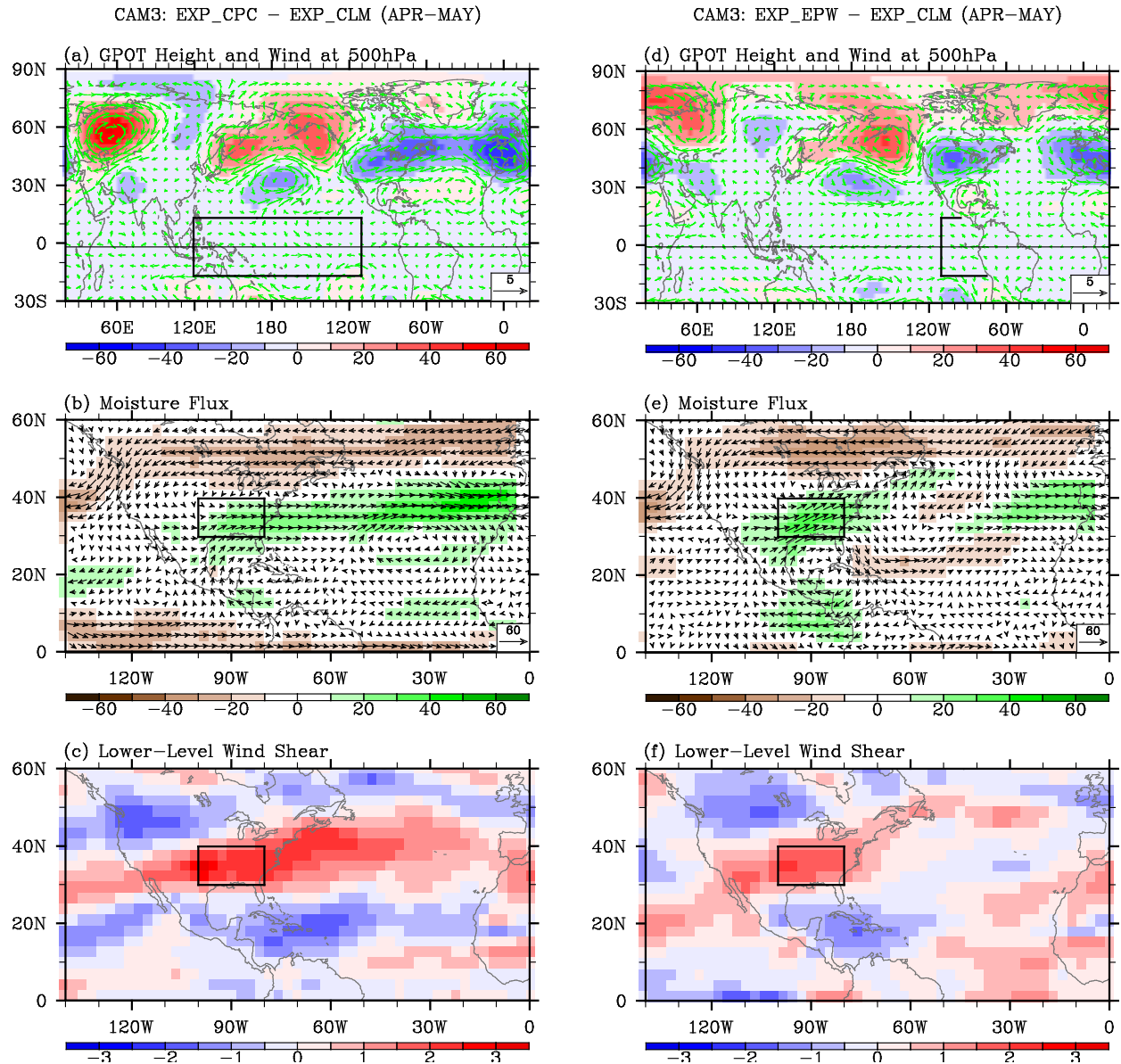


**Figure 8.** Simulated anomalous geopotential height and wind at 500 hPa, moisture transport, and lower-level (500 hPa – 925 hPa) vertical wind shear in AM obtained from EXP\_CPC – EXP\_CLM (a, b and c), and EXP\_EPW – EXP\_CLM (d, e and f). The units are  $\text{kg m}^{-1} \text{sec}^{-1}$  for moisture transport, m for geopotential height, and  $\text{m s}^{-1}$  for wind and wind shear. Thick black lines in (a) and (d) indicate the regions where the model SSTs are prescribed. The small box in (b), (c), (e) and (f) indicates the central and eastern U.S. region frequently affected by intense tornadoes.

CAM3: Convective Precipitation (APR-MAY)

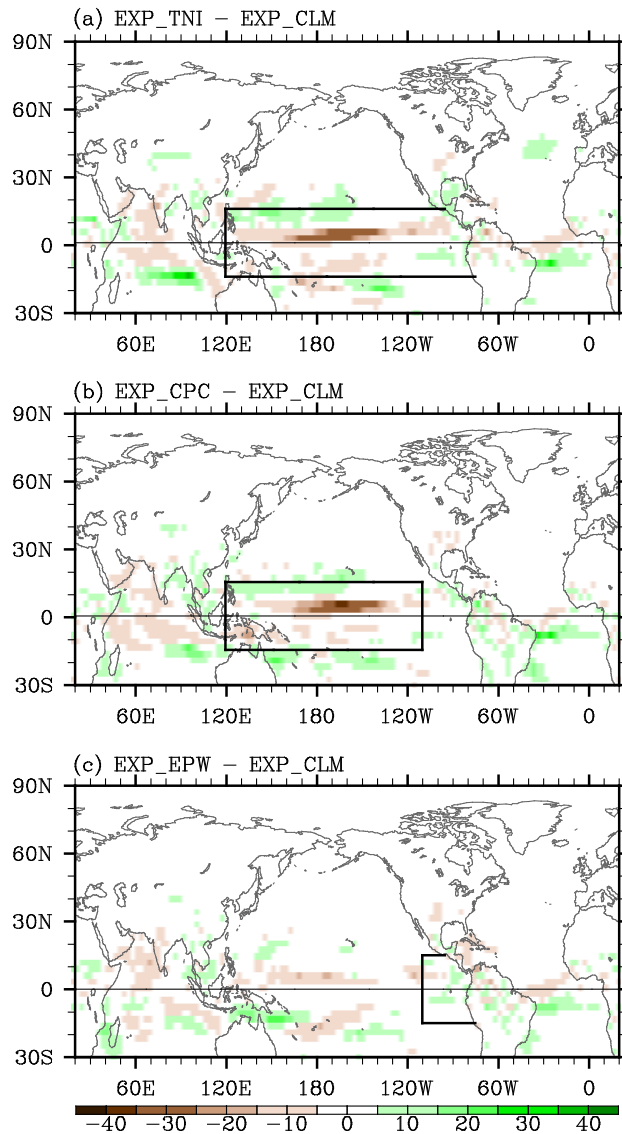


**Figure 9.** Simulated anomalous convective precipitation rate in AM obtained from (a) EXP\_TNI - EXP\_CLM, (b) EXP\_CPC - EXP\_CLM, and (c) EXP\_EPW - EXP\_CLM. The unit is  $\text{mm day}^{-1}$ . Thick black lines in (a) - (c) indicate the tropical Pacific region where the model SSTs are prescribed.

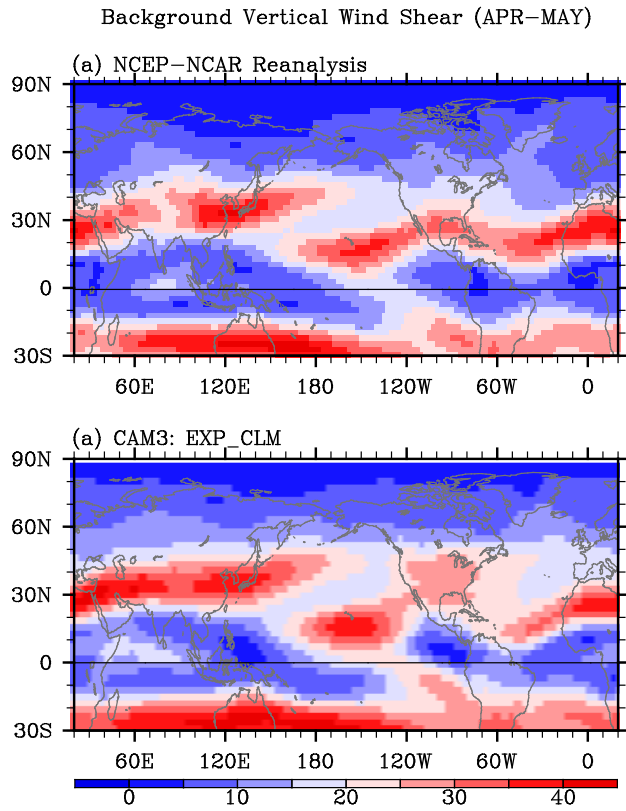


**Figure 10.** Background (climatological) vertical wind shear between 200 and 850 hPa in AM obtained from (a) NCEP-NCAR reanalysis, and (b) EXP\_CLM. The unit is  $\text{m sec}^{-1}$ .

ERSST3: 2011 (APR-MAY)

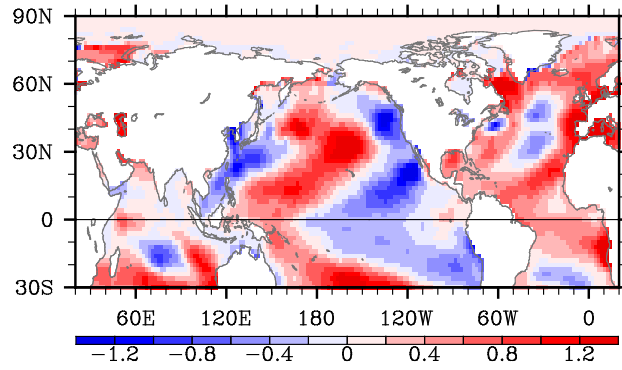


**Figure 11.** Anomalous SST in AM of 2011 obtained from ERSST3. The unit is °C.



NCEP-NCAR Reanalysis: 2011 (APR-MAY)

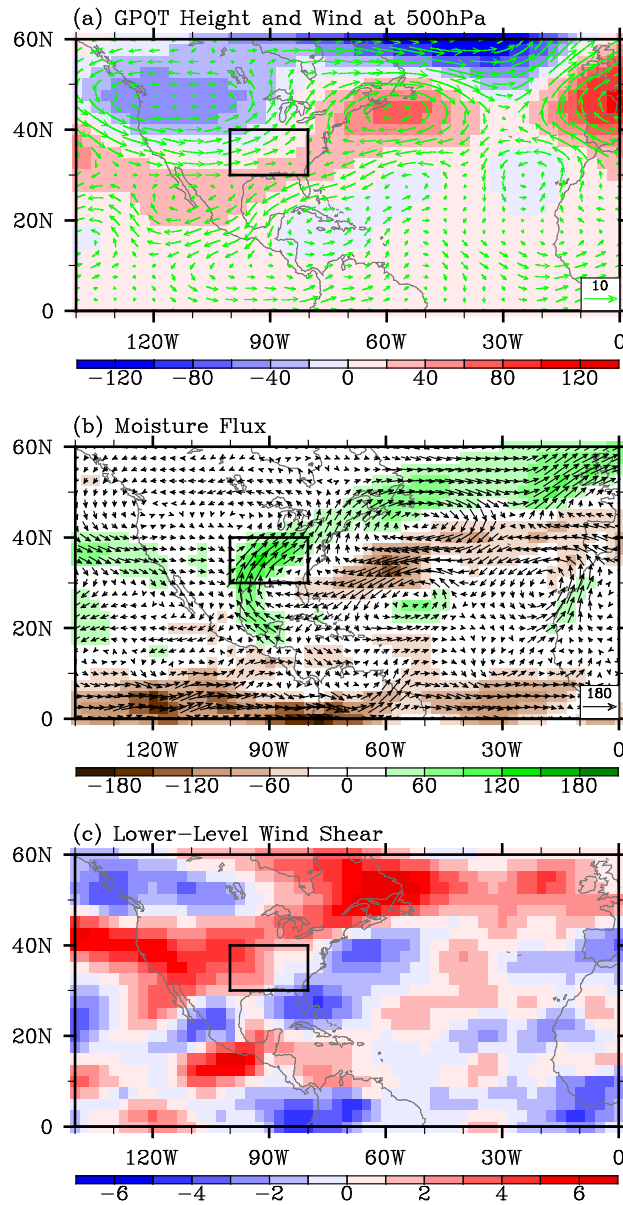


**Figure 12.** Anomalous (a) geopotential height and wind at 500 hPa, (b) moisture transport and lower-level (500 hPa – 925 hPa) vertical wind shear in AM of 2011. The moisture transport, geopotential height, wind and wind shear are obtained from NCEP-NCAR reanalysis. The unit is  $\text{kg m}^{-1} \text{sec}^{-1}$  for moisture transport, m for geopotential height, and  $\text{m s}^{-1}$  for wind and wind shear. The small box in (a), (b) and (c) indicates the central and eastern U.S. region frequently affected by intense tornadoes.



CAM3: EXP\_011 – EXP\_CLM (APR–MAY)

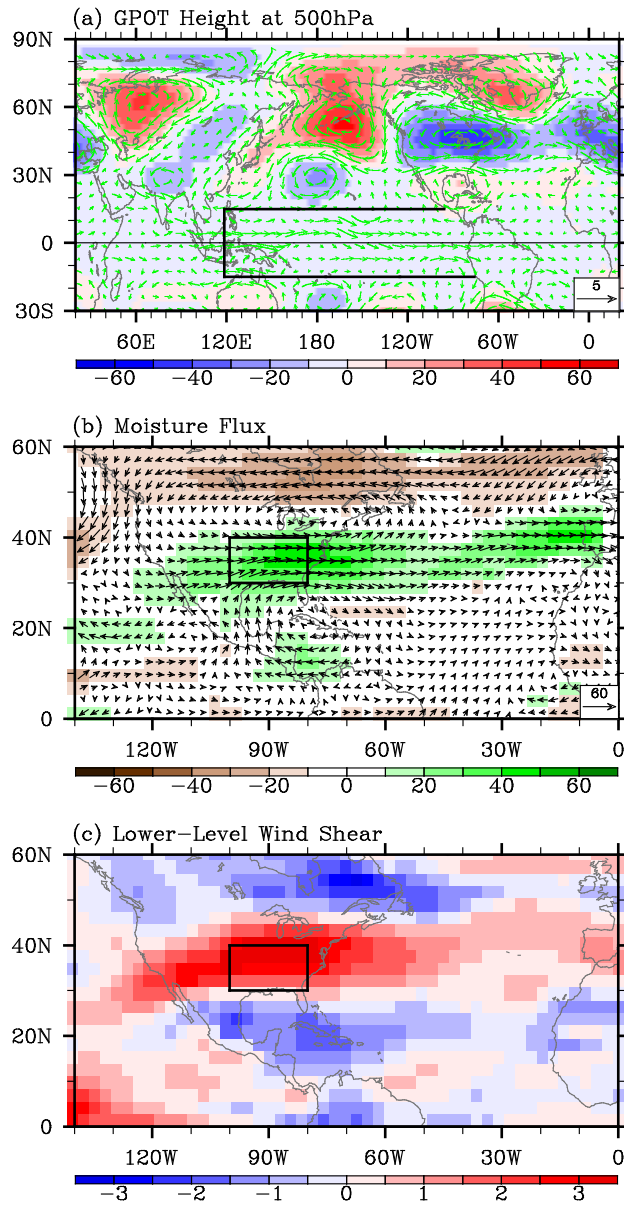


**Figure 13.** Simulated anomalous (a) geopotential height and wind at 500 hPa, (b) moisture transport and (c) lower-level (500 hPa – 925 hPa) vertical wind shear in AM obtained from EXP\_011 – EXP\_CLM. The unit is  $\text{kg m}^{-1} \text{sec}^{-1}$  for moisture transport, m for geopotential height,  $\text{m s}^{-1}$  for wind and wind shear. Thick black lines in (a) indicate the tropical Pacific region where the model SSTs are prescribed. The small box in (b) and (c) indicates the central and eastern U.S. region frequently affected by intense tornadoes.

CAM3: EXP\_WPW – EXP\_CLM (APR–MAY)

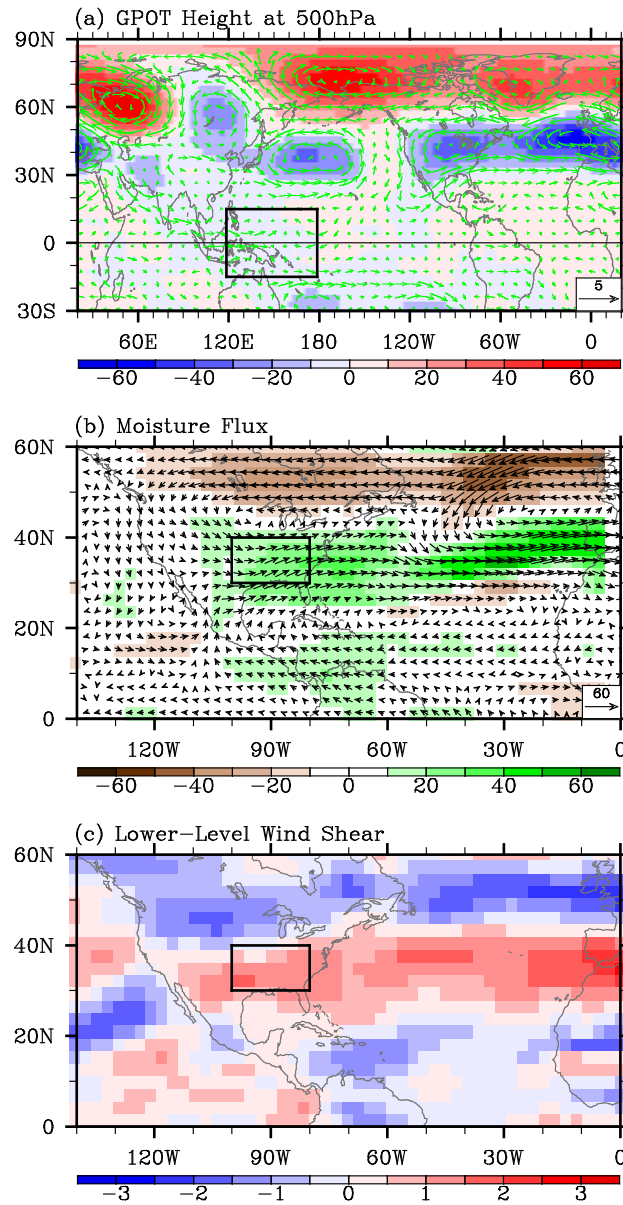


**Figure 14.** Simulated anomalous (a) geopotential height and wind at 500 hPa, (b) moisture transport and (c) lower-level (500 hPa – 925 hPa) vertical wind shear in AM obtained from EXP\_WPW – EXP\_CLM. The unit is  $\text{kg m}^{-1} \text{sec}^{-1}$  for moisture transport, m for geopotential height,  $\text{m s}^{-1}$  for wind and wind shear. Thick black lines in (a) indicate the tropical Pacific region where the model SSTs are prescribed. The small box in (b) and (c) indicates the central and eastern U.S. region frequently affected by intense tornadoes.

CAM3: Convective Precipitation (APR–MAY)

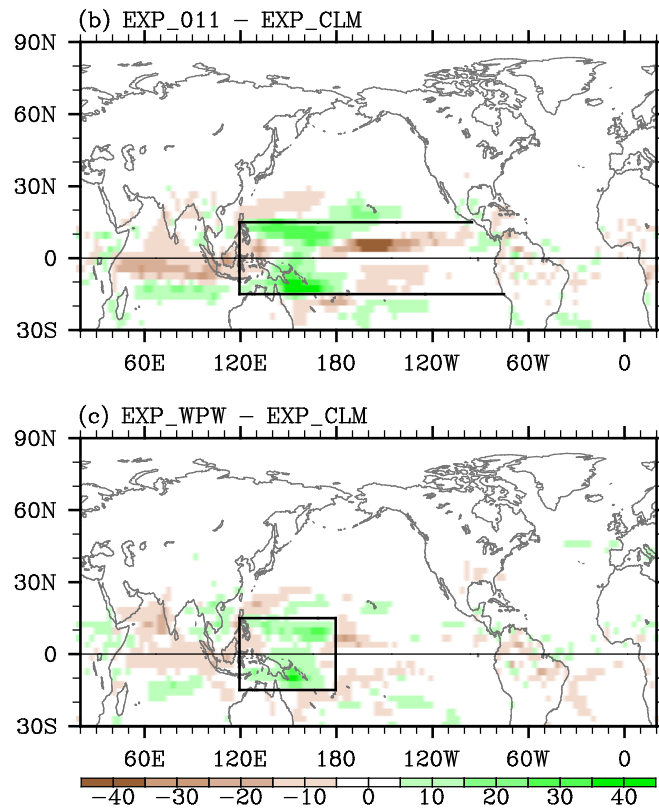


**Figure 15.** Simulated anomalous convective precipitation rate in AM obtained from (a) EXP\_011 - EXP\_CLM, and (b) EXP\_WPW - EXP\_CLM. The unit is  $\text{mm day}^{-1}$ . Thick black lines in (a) and (b) indicate the tropical Pacific region where the model SSTs are prescribed.